JOURNAL OF MATERIALS SCIENCE 11 (1976) 2004–2014

Adhesion of epoxy resins to metals

Part 1

E. H. ANDREWS, N. E. KING*
Department of Materials, Queen Mary College, London, UK

The adhesion of an epoxy resin above its glass transition temperature to aluminium, steel and gold surfaces has been studied using the methods of fracture mechanics. The results are compared with those of a previous study of elastomeric adhesives by Andrews and Kinloch, and the "intrinsic failure energies", θ_0, for the epoxy–metal bonds are deduced by similar methods. Correspondence, within a factor of two, is found between θ_0 and the thermodynamic work of adhesion, w_A, for most cases of interfacial failure, indicating both the absence of specific or chemical interactions at the interface and a purging of surface contaminants by the epoxy. An exception occurs when an excess of epoxy groups exist in the uncured resin. Here, for steel and aluminium but not for gold, the interfacial bonding is stronger than the cohesive strength of the resin due probably to the formation of strong bonds with the metal oxide surface layer.

1. Introduction

In the previous work of Andrews and Kinloch [1–4] fracture-mechanics methods were employed to obtain the adhesive failure energy, θ, for an elastomeric adhesive bonded to various plastic substrates. This quantity was found to obey the theoretical fracture equation of Andrews [5] which for adhesive failure, takes the form

$$\theta = \theta_0 \Phi(\dot{c}, T, \epsilon_0) \quad (1)$$

where θ_0 is the "intrinsic failure energy" and represents the energy required to break unit area of interatomic bonds across the fracture plane. In the simple case of interfacial failure, θ_0 is the thermodynamic work of adhesion of the interface. The "loss-function" Φ is a function of the rate of crack propagation, $\dot{c}$, the temperature T and ϵ_0, the strain in the elastomer remote from the propagating crack.

In the case of elastomeric adhesives, the loss function Φ is simplified because its rate and temperature dependence can be combined by means of the WLF time–temperature superposition procedure and

$$\Phi \equiv \Phi(\dot{c}a_T, \epsilon_0) \quad (2)$$

where a_T is the shift factor. This procedure is invalid for polymeric adhesives which are glassy or crystalline and thus for epoxy resin adhesives below their glass transition temperatures. Above T_g, however, the thermosetting epoxies are elastomeric and it is found that they can be treated by exactly the same analysis used previously for elastomers.

The particular advantage of this approach is that reliable values can be deduced for the intrinsic failure energy θ_0. Since this quantity relates to the atomic bonding across the fracture plane it provides important information about the nature of this bonding which is, of course, unchanged by passage through the glass transition.

2. Materials and specimen preparation

The epoxy resin used was a diglycidyl ether of bisphenol A of molecular mass ~370 obtainable as "Shell 828". The hardener ("Shell 114") was a blend of two cycloaliphatic amines with added benzyl alcohol as an accelerator.

The stoichiometric mixture of these components is obtained using a mass ratio of resin to hardener of 5 to 2. This mixture gives a cured

* Present address: Corporate Research and Development, Metal Box Ltd, Twyford Abbey Road, London, UK.

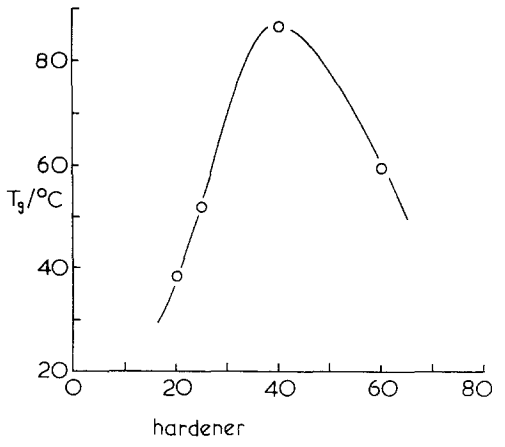

Figure 1 Glass transition temperature as a function of hardener content (expressed as parts per hundred of resin) for "Shell 828" epoxy resin.

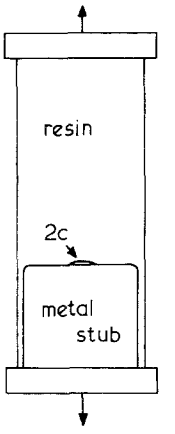

Figure 2 Simple-extension adhesive test specimen incorporating a preformed crack of length 2*c*.

resin of maximum glass transition temperature. To explore the effect of varying the hardener content, other ratios were also used, namely 5/1, 5/1.25 and 5/3. The effect of hardener content on T_g of the cured resins is shown in Fig. 1.

The metal substrates were prepared in the form of thin square plates ("Stubs") with two rounded corners. The surface to be bonded was the plate edge between the rounded corners and this was prepared in the following ways.

The aluminium and stainless steel stubs were machined, degreased in acetone and trichloroethylene, and finally etched before bonding. The aluminium stubs were treated as per ASTM D 2651; after degreasing, the stubs were immersed in an etching solution for 10 min at a temperature in the range 65 to 68° C. The etching solution consisted of sodium dichromate, sulphuric acid and deionized water in the weight ratio 1 : 10 : 30 respectively. The stubs were rinsed in running tap water and finally dried for 1 h at 60° C in a forced air oven. The adhesive joints were formed within 4 h of preparing the adherend surface.

The stainless steel stubs were treated as per Muchnick [16] and Ciba Geigy A15 [7]; after degreasing, the stubs were immersed in an etching solution for 15 min at a temperature in the range 49 to 54° C. The etching solution consisted of 35 ml saturated sodium dichromate solution dissolved in 1 litre concentrated sulphuric acid. The stubs were rinsed in running tap water before drying at 80° C in a forced air oven for 30 min, and the adhesive joints were formed within 4 h of preparing the adherend surface.

The gold substrates were prepared by electroplating copper stubs to provide a thickness of 5 μm of gold.

The adhesive test specimens were of the form illustrated in Fig. 2 and are identical to the simple-extension specimens described by Gent and Kinloch [8] and employed by Andrews and Kinloch [1] for elastomeric adhesives. The test specimens were prepared in the following manner.

The resin and hardener were outgassed and heated at 70° C in a vacuum oven. This procedure was followed in order to prevent bubbles forming during mixing, and also to improve the mixing. The hardener was added to the resin, mixed and finally poured into open top moulds, each one containing one of the metal stubs. The testpieces were left to gel at ambient temperature for 4 h, then postcured for $15\frac{1}{2}$ h at 120° C. The specimens were left in the oven which was cooled at a rate of approximately 15° C h^{-1}.

The initial crack at the interface was obtained by masking off the surface to be bonded except for a central section of length equal to the crack length required. This exposed section was sprayed with an aerosol mould-release agent containing PTFE, and the masking removed. Since the epoxy does not adhere to the sprayed region, the latter serves as an initiator crack in the finished specimen.

3. Surface preparations

One parameter of major interest is the condition of the substrate surface prior to bonding. It is well known that high energy surfaces like metals and metal oxides, adsorb from the atmosphere a layer of hydrocarbon contamination which drasti-

TABLE I Contact angles of liquid drops on the metal surfaces

	Before treatment	After ultra-violet ozone treatment
Water	$>90°$	20°
Glycerol	46°	5°
1-bromonaphthalene	22°	0°

cally reduces the effective surface energy. Such contaminant layers are difficult to remove, and reform rapidly. Clearly, the presence or absence of such a layer should profoundly modify the quantity θ_0 and thus the adhesive strength of the interface.

In order to study this question, some of the metal substrate surfaces were subjected to a purging treatment of known effectiveness. This consisted in exposure to intense ultra-violet radiation in an air flow [9]. The ultra-violet radiation produces ozone which, in the simultaneous presence of the radiation itself, degrades and oxidizes the contaminant hydrocarbons.

Typical purging conditions employed in these tests involved exposure to a bank of six 4 W ultra-violet lamps in an air flow of $1.56 \times 10^3 \text{ cm}^3 \text{sec}^{-1}$ for a period of up to 2 days. The effectiveness of the treatment was monitored by measuring the contact angles of liquid drops on the metal surfaces, typical data for gold surfaces being as shown in Table I.

Of course, for atomically clean surfaces of metal or oxide, the contact angle should reduce to zero even for water which should, therefore, spread. These conditions were not achieved, but the drastic reductions in contact angle obtained suggest that some areas of the surface were being effectively purged. This should result in a corresponding increase in the thermodynamic work of adhesion of any adhesive joint made promptly after the purging treatment.

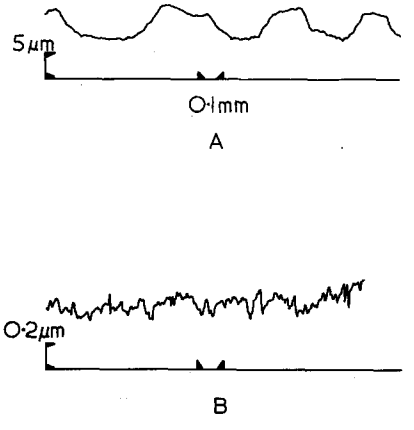

Figure 3 "Talysurf" roughness profiles for stainless steel specimens. (A) normal surface; (B) highly polished surface.

The effect of surface roughness was investigated for steel specimens by polishing to varying degrees. The "normal" surface finish (6 μm roughness) is compared in Fig. 3 with a highly polished finish (600 grade paper 0.2 μm roughness) by means of their "Talysurf" traces. Both types of surface were used in the experimental study.

4. Testing procedures

Testing was carried out in the temperature control cabinet of an Instron testing machine and over a temperature range of 45 to 170° C. One tip of the artificial crack was observed by means of a cathetometer containing an eyepiece graticule. When the crack propagated, its growth could be timed over a fixed distance (usually 1 mm) on the graticule scale, providing an average initial crack velocity, $\dot{c}$.

The specimen itself was extended in tension at a selected cross-head speed until crack propagation was observed. The load–deflection curve was recorded meanwhile and the onset of crack propagation was noted on the curve by manual operation of an "event marker". The area under the load–deflection curve, divided by the volume of the epoxy sheet, gives the average input strain-energy density. Strictly speaking this quantity only equals the input energy density, W_0, remote from the crack, when no crack is present. However, the load–deflection curves for specimens containing cracks and for uncracked specimens are indistinguishable in practice, so that W_0, and its critical value W_{0c} for the onset of crack propagation, can be deduced directly in each experiment.

Cross-head speeds ranging from 0.01 to 0.5 cm min^{-1} were employed, the higher speeds normally giving larger initial growth rates $\dot{c}$ at a given temperature. The procedure described for measuring $\dot{c}$ is adequate for tests above T_g, results of which are presented in this paper. For tests below T_g crack propagation is often too rapid for visual measurement of $\dot{c}$ and in these cases an electrical resistance method was used instead. This will be described elsewhere.

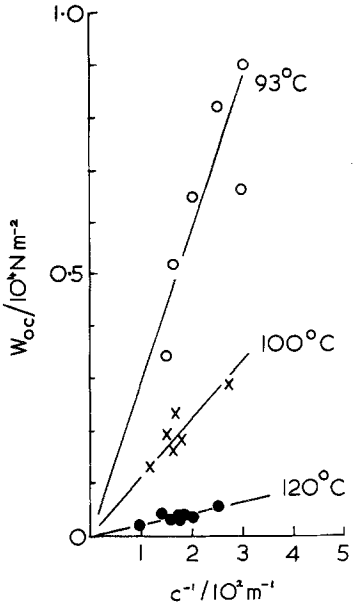

Figure 4 Critical energy densities for fracture, W_{0c}, plotted against reciprocal crack length for the 5/2 resin at three different temperatures.

5. Results

5.1. Analysis

The adhesive failure energy θ was obtained using the following formula [1], which is valid for inelastic materials as shown in [5].

$$\theta = kcW_{0c}. \tag{3}$$

The strain in the epoxy resin at which crack propagation occurred was always less than 5%, and under these circumstances $k \sim \pi$. Fig. 4 shows typical plots of W_{0c} versus c^{-1}, confirming the validity of Equation 3 and providing slopes for which θ is immediately deducible.

Before plotting θ as a function of rate and temperature, the WLF transform was applied to give the reduced rate of crack propagation $\dot{c}a_T$, where

$$\log a_T = \frac{C_1(T-T_g)}{C_2+T-T_g} \tag{4}$$

using the conventional "universal" values of $C_1 = 17.4$ and $C_2 = 51.6$ K.

Similar data, but for cohesive fracture of the resins alone, give the surface work $\mathcal{T}$ as a function of reduced rate and have been reported elsewhere for the resins used in this study [10]. Since θ refers to unit area of interface, and $\mathcal{T}$ to unit area of crack surface, comparison applies between θ and $2\mathcal{T}$, one interface corresponding to two surfaces after separation. (Note that in Andrews and Kinloch [1] the symbol $\mathcal{T}$ is referred to unit area of interface and thus corresponds to $2\mathcal{T}$ in this paper and in [5].)

For a sheet of adhesive bonded to a rigid substrate [4]

$$\begin{aligned} 2\mathcal{T} &= 2\mathcal{T}_0\Phi(\dot{c}, T, \epsilon_0) \\ \theta &= \theta_0\Phi(\dot{c}, T, \epsilon_0) \end{aligned} \tag{5}$$

where $\mathcal{T}_0$ is the intrinsic energy for cohesive failure of the adhesive and Φ is the same loss function for both cases. Thus

$$\theta_0 = \theta\mathcal{T}_0/\mathcal{T}. \tag{6}$$

Values of $2\mathcal{T}_0$ for the resins employed here have been obtained theoretically in another paper and confirmed experimentally in the case of one of them. These values are given below:

Resin (epoxy/hardener)	5/1	5/1.25	5/2	5/3
$2\mathcal{T}_0$ (mJ m^{-2})	4050	3050	2590	2830

4.2. Reduced-rate dependence of θ

Fig. 5 shows $\log\theta$ plotted against $\log \dot{c}a_T$ for the 5/2 epoxy bonded to the Al substrate. The data

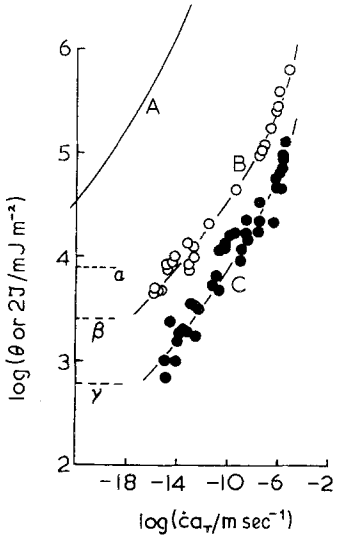

Figure 5 Adhesive failure energy, θ, and cohesive failure energy, $2\mathcal{T}$, as functions of the reduced rate of crack propagation. (A) Cohesive failure energy for styrene-butadiene rubber [1]; (B) cohesive failure energy for the 5/2 epoxy resin; (C) adhesive failure energy for the 5/2 epoxy resin bonded to aluminium. The corresponding intrinsic failure energies $2\mathcal{T}_0$ (SBR), $2\mathcal{T}_0$ (epoxy) and θ_0 (epoxy–Al) are shown at α, β and γ respectively.

for $\log 2\mathcal{T}$ are also included as is the curve obtained by Andrews and Kinloch for cohesive failure of SBR rubber. The dependence of θ upon reduced rate is, of course, a consequence of the loss function Φ, and this appears to be quite similar in form for the epoxy and for SBR. The much higher values of $2\mathcal{T}$ for SBR are largely a consequence of the higher $2\mathcal{T}_0$ value for this material, namely 8.32×10^3 compared to $2.6 \times 10^3\,\mathrm{mJ\,m^{-2}}$ for the epoxy. The remaining discrepancy could be explained by a shift of the data along the $\dot{c}a_T$ axis, i.e. by a difference in the reduced rate at which Φ falls to its limiting value of unity. This limit appears to occur at lower reduced rates for SBR than for the epoxy resins.

The curve for adhesive failure is parallel, within experimental error, to that for cohesive failure in the epoxy, in the sense that the two curves can be superimposed by shifting along the $\log\theta$ axis. This is in complete harmony with the findings of Andrews and Kinloch for a SBR adhesive bonded to plastic substrates and with the theoretical relationship (Equation 1) which can be re-written

$$\begin{aligned} \log\theta &= \log\theta_0 + \log\Phi \\ \log 2\mathcal{T} &= \log 2\mathcal{T}_0 + \log\Phi. \end{aligned} \tag{7}$$

The vertical displacement of the curves is, of course, the quantity $\log(2\mathcal{T}_0/\theta_0)$ whence, using the values given earlier for $2\mathcal{T}_0$ we obtain

$$\theta_0 = 580\,\mathrm{mJ\,m^{-2}}$$

for the 5/2 epoxy bonded to the Al substrate. The complete data for θ_0 is given in Table II and will be discussed later.

Within experimental error, the behaviour of θ for the 5/2 epoxy is independent of the substrate.

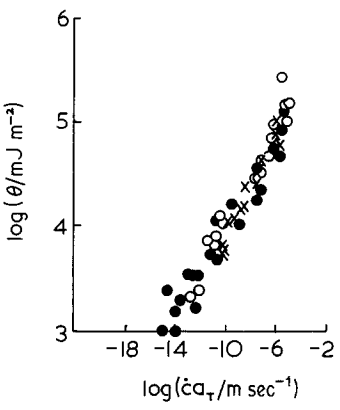

Figure 6 Adhesive failure energies, θ, for the 5/2 epoxy bonded to aluminium (•), steel (○) and gold (×).

This is shown in Fig. 6 where points for Al, steel and gold substrates are seen to lie on a single curve. It was, of course, expected that Φ would be independent of substrate, but these data show that θ_0 is also unaffected by the adherends even though one is a noble metal and the others are oxidized surfaces. This result will be discussed presently.

Fig. 7 shows the data for the surfaces cleaned by UV/ozone treatment. Once again both Φ and θ_0 are unchanged as a result of this treatment and this will be discussed more fully below.

Finally, for the 5/2 epoxy, Fig. 8 shows that reducing the surface roughness from $6\,\mu m$ to $0.2\,\mu m$ on steel specimens produces no change in θ and thus no change in Φ or θ_0. This may seem strange at first, but examination of the "Talysurf" traces suggests that although polishing reduces the scale of the surface relief, the "true area" or trace contour length is relatively unaffected. This can

TABLE II θ_0 and $2\mathcal{T}_0$ values ($\mathrm{mJ\,m^{-2}}$)

Substrate	Resin			
	5/1	5/1.25	5/2	5/3
Cohesive $2\mathcal{T}_0$ (calculated)	4050	3050	2590	2830
(expt.)	3700		< 3800	
Steel, etched	7820*		700	715
unetched			850	
polished			765	
ultra-violet/ozone			680	
Aluminium, etched	⩾ 4050		580	
Gold, plated	1350		800	715
ultra-violet/ozone			600	

* From four interfacial data points; fracture was otherwise cohesive showing $\theta_0 \geqslant 4050$.
Note: reproducibility of θ_0 and $2\mathcal{T}_0$ is not better than ± 10%.

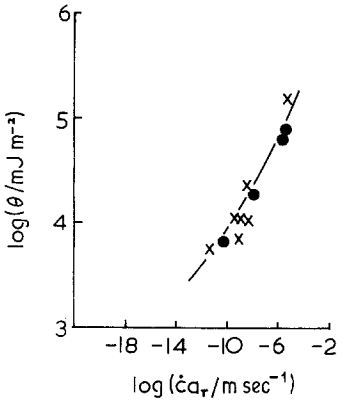

Figure 7 Adhesive failure energy, θ, for the 5/2 epoxy bonded to metal surfaces cleaned by ultra-violet/ozone treatment; (•) steel. (X) gold; the solid curve is the relation for untreated surfaces.

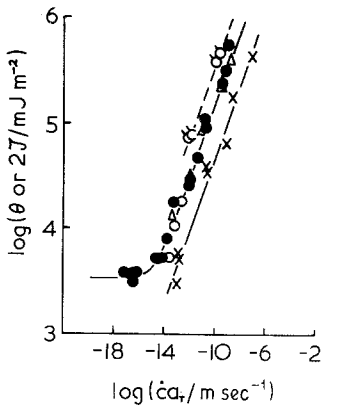

Figure 9 Adhesive failure energy, θ, and cohesive failure energy, $2\mathcal{J}$, for the 5/1 epoxy resin: (•) cohesive, resin alone; (ȣ) θ for steel substrate, interfacial failure; (○) θ for steel substrate, "cohesive" failure; (△) θ for aluminium substrate, all cohesive; (X) θ for gold substrate, all interfacial failure.

be better envisaged by realizing that a saw-tooth surface profile with a 45° pitch will always have a contour length $\sqrt{2}$ times the corresponding planar distance regardless of the absolute height of the saw-teeth. It is very difficult, therefore, by normal surface preparation methods to change the true surface area by more than a factor of two, and this probably explains the relative insensitivity of $\log\theta$ to surface finish.

5.3. Variation of the hardener content

Figs. 9 and 10 show $\log\theta$ versus $\log \dot{c}a_T$ plots for the resins containing respectively less and more hardener than the 5/2 stoichiometric proportion. All curves are reduced to T_g by the WLF procedure, thus eliminating the effect of T_g variations.

Results for the 5/3 epoxy (excess hardener) are in all ways similar to those for the 5/2 resin. The cohesive failure curve ($\log 2\mathcal{J}_0$) lies above, but parallel to, the adhesive failure curves. Again, the data for different substrates (only gold and steel were tested for this resin) are indistinguishable.

Significant variations in behaviour are found for the 5/1 epoxy, as Fig. 9 reveals. Firstly, the cohesive failure curve in this case is significantly different, being steeper than those of the other resins and also revealing an abrupt transition at low reduced rate to a constant value independent of crack speed and temperature. The cohesive failure energies of these resins are discussed more fully elsewhere, but it appears that this transition reflects the onset at low $\dot{c}a_T$ of a truly elastic

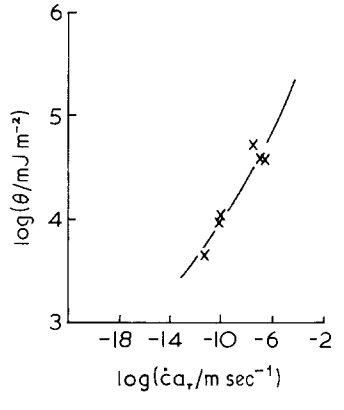

Figure 8 Adhesive failure energy, θ, for the 5/2 epoxy bonded to normal steel surfaces (solid line) and highly polished steel surfaces (points).

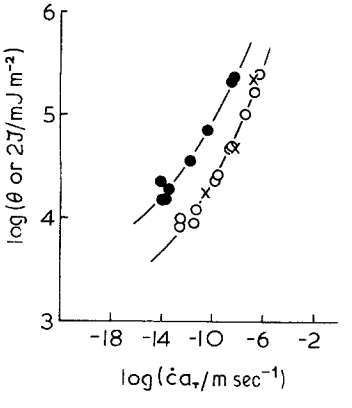

Figure 10 Adhesive failure energy, θ, and cohesive failure energy, $2\mathcal{J}$, for the 5/3 epoxy resin: (•) cohesive; (○) θ for steel substrate; (X) θ for gold substrate.

regime ($\Phi \rightarrow 1$) and that the recorded value of $2\mathcal{T}$ is equal to the intrinsic failure energy $2\mathcal{T}_0$. The experimental value of this limit, $2\mathcal{T}_0 = 3700$ mJ m^{-2}, corresponds quite closely with a theoretical estimate of 4050 mJ m^{-2}.

Turning to the adhesive failure results we now find that only the gold substrate gives a curve lying below and parallel to the cohesive failure curve. For both steel and Al substrates, most of the failures were not interfacial, the crack propagating immediately through the resin at an angle of some 30°, suggestive of propagation along a locus of maximum shear stress. The data for $\log\theta$ in these cases fell uniformly on the cohesive failure curve (Fig. 9), as is to be expected. In just four experiments, however, using steel substrates and at higher reduced rates, interfacial propagation was obtained over short distance and these points (shown by the symbol, ♭ in Fig. 9) define a curve which actually lies above the cohesive failure curve i.e. the interface θ_0 value exceeds the cohesive $2\mathcal{T}_0$ value.

It is difficult to see why, in this situation, interfacial failure is observed at all, since the interface is stronger than the epoxy. That occasional experiments do show this effect is possibly due to the location at the interface of the initial artificial flaw with its extremely fine crack tip defined, of course, by the thickness of the sprayed PTFE layer. This confines the highest stress concentration to a very narrow interfacial region, causing preferential failure at the stronger interfacial bonds. As the crack grows and the tip stress-field enlarges, the weaker cohesive bonds are subjected to higher stresses until they now fail in preference to the interfacial bonds and the crack branches away from the interface.

It thus appears that θ_0 for the 5/1 epoxy bonded to oxidized substrates exceeds the intrinsic cohesive failure energy $2\mathcal{T}_0$, but that θ_0 for the noble metal follows the more normal pattern established for elastomeric systems and the other epoxies in which adhesive bonding is weaker than the polymer network itself.

The most likely origin of the specific interactions occuring between the 5/1 resin and the metal surfaces (giving high θ_0 values) involves the presence of OH groups on the substrate surfaces. The 5/1 resin differs from the other resins used in having an excess of unreacted epoxy groups in the cured resin.

With appropriate catalysation [11], these excess epoxy groups can react with the hydrated metal oxide surfaces to produce an ether type chemical bond across the interface. Some possible mechanisms are:

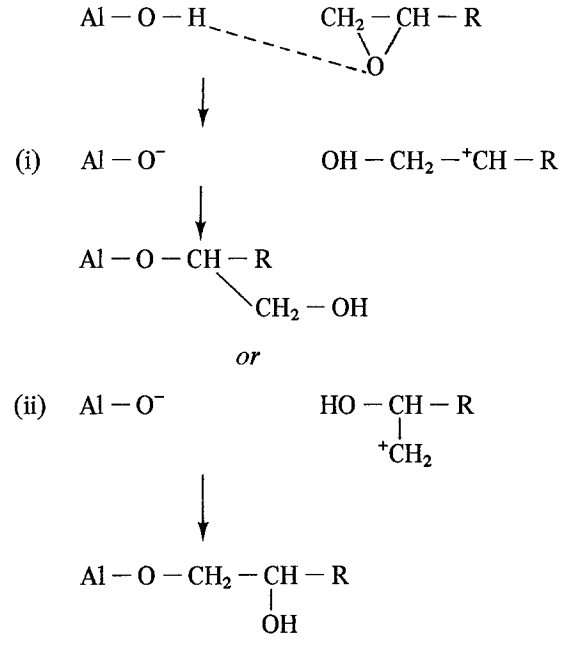

Other acid catalysed and base catalysed reactions can also be envisaged. MacDonald and Hayes [18] have shown that oxygen can be adsorbed in small quantities on gold surfaces at room temperature. It is thus possible that a similar reaction may occur to a smaller extent with the 5/1 epoxy bonded to gold giving θ_0 values higher than those obtained for the 5/2 and 5/3 resins against gold.

5.4. Thermodynamic work of adhesion

In the earlier work of Andrews and Kinloch, on elastomers bonded to plastic substrates, the values deduced for θ_0 agreed closely with the thermodynamic work of adhesion w_A provided failure was interfacial. It is, therefore, of interest to see if a similar correspondence applied in the present experiments.

The method used to measure w_A in the earlier studies were fully described therein [1] and involved the determination of contact angles for various liquid pairs on both adhesive and substrates solids. The same procedure has been followed here but is subject to serious errors because the substrates are now solids of intrinsically high

surface energy. The problem did not arise in the earlier work because, there, both adhesive and adherend were organic solids of low surface energy.

It has been shown clearly by Harkins and Loesner [12] that the thermodynamic work of adhesion is given by an equation of the form

$$w_A = \pi_e + \gamma_L(1 + \cos\phi)$$

where π_e is the "spreading pressure" and equals the decrease in the surface free energy of the solid on immersion of the solid in the saturated vapour of the liquid; γ_L is the surface energy of the liquid and ϕ the contact angle.

In the procedure of Kaelble [13] used in [1], the spreading pressure π_e is neglected in the computation of the polar and dispersive contributions to w_A, this approximation being valid as long as γ_{LV} (interfacial energy between liquid and its saturated vapour) is much greater than the critical surface energy γ_c for wetting of the solid [14]. This condition is fulfilled for organic liquids in contact with organic solids ($\gamma_s < 100\,mJ\,m^{-2}$), but fails when the substrate has a high energy surface ($\gamma_s > 500\,mJ\,m^{-2}$).

Unfortunately, π_e values are not available for the systems used in the present study. The use of "typical" values for π_e for organic vapours on metal and oxide surfaces (30 to $40\,mJ\,m^{-2}$) suggests that the w_A values obtained ignoring π_e may be too low by up to 30% to 50%. This accords with the data of Harkins and Loesner who found that π_e could contribute as much as half the true value of the work of adhesion for organic vapour/metal systems.

The collected data for θ_0 and w_A are given in Table III. For etched and ultra-violet/ozone treated surfaces, the w_A values were obtained from our own measurements [19] and ignore π_e. They are likely, therefore, to be low by a factor of up to two and the figures bear an asterisk to denote this. For atomically clean metal surfaces, values of γ_s^D and γ_s^P (the dispersive and polar contributions respectively to the surface free energy of the substrate) have been taken from the literature [19]. The w_A values derived from these data are not subject to errors caused by neglecting π_e.

Referring to Table II we see firstly that θ_0 for the 5/1 epoxy is, in all cases, greatly in excess of the thermodynamic work of adhesion, even for clean metal surfaces. This clearly indicates the formation of strong bonds between this resin and the metal surfaces. There is a noticeable difference between the oxide surfaces of Al and steel, where the interfacial bond is stronger than the cohesive bonding of the resin, and the noble metal surface where it is weaker. Nevertheless, even for gold, θ_0 is a factor of two greater for the 5/1 resin than for either the 5/2 or 5/3 compositions.

Consider next the very small difference between the measured w_A figures for normal and ultra-violet/ozone treated surfaces. The dramatic changes obtained in the contact angle indicates that low energy contaminants *are* being removed by the treatment, yet the change in w_A fails to reflect this fact. This can be explained by the neglect of π_e, since this quantity must be considerably higher for the cleaned surface than the normal surface. Another way of expressing this is to say that the atmospheric contaminants removed by treatment are being replaced by an adsorbed layer of the test liquid, whose contact angle is being measured. Thus we expect the true value of w_A for treated surfaces to be up to twice that

TABLE III θ_0 and w_A values ($mJ\,m^{-2}$)

Substrate	Resin					
	5/1		5/2		5/3	
	θ_0	w_A	θ_0	w_A	θ_0	w_A
Steel, etched	7820	–	700	–	715	–
ultra-violet/ozone	–	–	680	–	–	–
atomically clean	–	–	–	306	–	276
Aluminium, etched	>4050	101*	580	103*	–	94
atomically clean	–	333	–	306	–	–
Gold, plated	1350	94*	800	98*	715	89*
ultra-violet/ozone	–	110*	600	110*	–	99*
atomically clean	–	396	–	360	–	325

* These values probably under-estimated by a factor of two. See text.

recorded in Table II whilst for the untreated surfaces, of relatively low energy, the w_A values as given may be only slightly in error. This would suggest that w_A for treated surfaces lies about half way between that for normal surfaces and atomically clean surfaces.

In spite of the obvious effectiveness of ultraviolet/ozone treatment, θ_0 is hardly affected by such preparation. The most obvious explanation of this is that the liquid epoxy resin is capable of desorbing and replacing the contaminant species on normal surfaces, producing direct secondary (or other) bonding with the metal or oxide substrate. Prior cleaning of the surface would not then be expected to reveal any advantage.

If this explanation is true (and it seems the only plausible explanation of the data) it suggests that the effectiveness of epoxy-resins as adhesives lies, at least partly, in their ability to purge surfaces of hydrocarbon contamination and bond directly with the clean substrate. It could also explain why hot-curing resins are generally more effective than cold-curing ones, in that the rates of diffusion and absorption will be enhanced by increased temperature.

The agreement, within a factor of two, between θ_0 and w_A (clean surfaces) for the 5/2 and 5/3 resins on all substrates, would seem to rule out the possibility of any specific or chemical interactions between these resins and the substrates. Only secondary bonds can exist if $\theta_0 \sim w_A$, since primary bonding would give $\theta_0 \gg w_A$.

That θ_0 is consistently about twice w_A (clean surfaces) for these two resins is probably not without significance in spite of uncertainties in the parameters used to calculate both quantities. One possible cause of the discrepancy is that θ_0 contains contributions from energy stored in those network chains actually attached to the surface. The large $2\mathcal{T}_0$ values for cohesive failure derive entirely from energy stored in the network chains [15] and it is possible that θ_0 is enhanced by a similar mechanism.

Assuming realistic values for the interatomic force constants for the bonds involved (co-valent in the network chain and Van der Waals at the interface itself), it can be shown that a contribution to θ_0 of only about $10^{-2} \times 2\mathcal{T}_0$ is to be expected from this cause, i.e. would predict $\theta_0 \sim 1.1\ w_A$ instead of $\sim 2w_A$ as observed. It is possible of course that the interfacial bond has a strong polar component and thus a force constant considerably higher than a simple secondary bond. To obtain $\theta_0 \sim 2\,w_A$ would require the interfacial bond to have a force constant as high as 0.2 times that of a covalent bond, which seems somewhat unlikely especially as θ_0 values for Al, steel and gold are virtually the same for the 5/2 and 5/3 resins.

An alternative cause of the high θ_0 values for these resins might be that strong bonds *are* formed at the interface at a small number of molecular attachment sites and that fracture is diverted into the resin phase in such vicinities. Adapting the formula of Andrews and Kinloch [2] for mixed-locus adhesive failure, and ignoring substrate failure, we have

$$\theta_0 = iw_A + r2\mathcal{T}_0$$

where i, r are respectively the fractional areas of interfacial and cohesive-in-resin failure ($i + r = 1$). To obtain $\theta_0 \sim 2w_A$ requires only that $r = 15$ to 19%, and an approximate experimental value for r of 0.11 ± 0.03 has been measured on an Al surface after debonding from the 5/2 epoxy using electron probe microanalysis [19]. Since strong bonds are obviously formed by the 5/1 resin (with excess epoxy groups) it is clearly possible that local variations in hardener content could give rise to small areas of enhanced bonding even in the 5/2 and 5/3 resins which have no overall excess of epoxy groups.

The occurrence of a certain amount of cohesive failure could also account for the scatter of the data for θ. This scatter is such that a lower bound curve (e.e. in Fig. 5) corresponds to a θ_0 value about half that obtained from the mean of the experimental points; θ_0 (lower bound) thus agrees closely with w_A and could represent the case where $r \to 0$, higher values of θ_0 occurring by fluctuations of r between zero and 20%.

5.5. The meaning of "interfacial failure"

It is generally held that epoxy resin-to-metal bonds never undergo truly interfacial failure [16] but that failure always occurs through the resin phase leaving a very thin layer of epoxy adhering to the metal. Indeed it has been asserted that no adhesive failure ever occurs by a genuinely interfacial separation [17].

Our earlier studies of elastomeric adhesives [1] show quite plainly that the latter assertion is wrong. True interfacial failure can and does occur when the atomic interaction across the interface

is limited to secondary bonding, even though the joint may be relatively strong. The locus of fracture is simply the line of least resistance, and the plane of secondary bonding is weaker, by orders of magnitude, than either of the cohesive phases.

If primary bonding can be established at the interface the situation is, of course, quite different and failure may occur in a wholly or partially cohesive mode. This also emerges clearly from the earlier work.

Epoxy resins tested above T_g are elastomeric and the results reported in this paper are very similar in general nature to those obtained previously with styrene butadiene rubber as the adhesive. The approximate identification of θ_0 with w_A in most cases indicates that failure here must also occur with a predominantly interfacial locus. Any large deviation from this would reveal itself immediately by an increase in θ_0.

This argument is modified somewhat by an effect that has not, to the authors' knowledge, been described previously. The formula for θ assumes that the substrate is rigid and that both energy supply and energy losses are confined to the half-plane occupied by the adhesive phase. This is strictly true only as long as the failure is completely interfacial.

Consider the diagram of Fig. 11a which shows the three cases of cracks propagating respectively at the interface, a small distance "above" the interface and a great distance from the interface. For the first case the bonding across the fracture plane is characterised by the interfacial θ_0. As soon as the fracture deviates, cohesively, into the adhesive phase, θ_0 is replaced by $2\mathcal{T}_0$, this change occurring without changes in the energy loss or supply pattern as long as the crack remains very close to the interface. A measurement of θ_0 under these conditions would give a value equal to $2\mathcal{T}_0$.

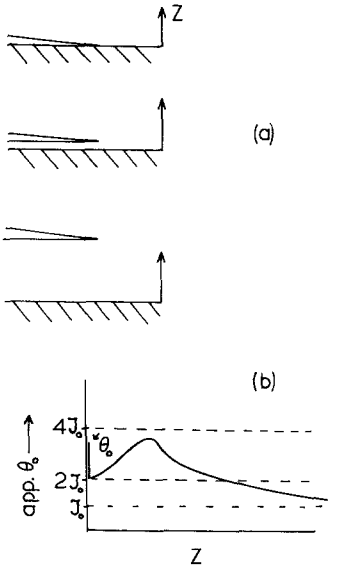

Figure 11 The effect of crack-to-interface separation on the apparent value of the intrinsic adhesive failure energy, θ_0.

As the distance, Z, between the interface and the fracture increases, part of the x-y plane below the fracture plane becomes involved both in the supply and loss of energy. Since energy loss predominates in the highly stressed "near field" and energy supply in the lightly stressed "far field", the value of θ will rise initially with increasing Z giving an apparent increase in θ_0 above the value of $2\mathcal{T}_0$ to some maximum not exceeding $4\mathcal{T}_0$. Of course, the atomic bonding is not increasing in strength with Z, and the increase in θ_0 is due to the formula for θ now being incorrect as events in the lower half-plane intervene. As Z increases further, energy losses in the lower half-plane are gradually compensated by energy supply from that region of the stress-field and θ decreases again. Eventually, of course, for $Z \to \infty$ we revert to the whole-plane cohesive situation in which the formula for θ gives $\theta_0 = \mathcal{T}_0$. In reality $\theta_0 = 2\mathcal{T}_0$ but the preceding result is a simple consequence of the fact that the formula for θ_0 takes account only of the energy supply from the upper half-plane.

These various possibilities are summarized in Fig. 11b where the values that would be deduced for θ_0 are plotted schematically against Z. At $Z = 0$, θ_0 is the value for interfacial bonding and is independent of the cohesive strength of the adhesive. If $\theta_0 < 2\mathcal{T}_0$, true interfacial failure will occur. As the crack moves marginally into the adhesive phase, an immediate change will occur to $\theta_0 = 2\mathcal{T}_0$ and this will normally result if θ_0 (interface) $> 2\mathcal{T}_0$. However, the fact that, at $Z > 0$, losses are encountered "below" the fracture plane means that the apparent value of θ_0 rises with increasing Z. There is, therefore, a tendency for the fracture plane to be "trapped" between the true interface and the maximum in the θ_0 versus Z curve. Generally this should result in value for θ_0 of the order of $2\mathcal{T}_0$, as was found for most steel and all Al data for the 5/1 resin. Occasionally, however, values as high as $4\mathcal{T}_0$ might be observed for a crack, strongly fugitive

from the interface, needing to pass over the maximum in the apparent θ_0 versus Z curve. This may provide an alternative explanation of the four experiments (for steel bonded to 5/1 epoxy) in which $\theta_0 > 2\mathcal{T}_0$ by a factor of 1.9. The effect here described could also account for the frequent reports of very thin layers of epoxy adhesives left on metal substrates after fracture. It should be emphasized, however, that data such as is given in this and preceding papers provides an unambiguous indication of whether failure is truly interfacial ($\theta_0 < 2\mathcal{T}_0$) or otherwise ($\theta_0 \geqslant 2\mathcal{T}_0$).

6. Conclusion

Applying fracture mechanics methods to epoxy resin-to-metal bonds above T_g of the resin provides data similar in general form to those previously obtained with elastomeric adhesives. In particular, the parallel configuration of curves for adhesive failure energy, θ, and cohesive failure energy, $2\mathcal{T}_0$, for the resin alone, confirms the adhesion theory advanced by Andrews and Kinloch, and allows the bond strength across the fracture plane to be deduced. This bond strength, expressed in terms of θ_0, the energy per area to fracture the bonds, is of the order of the thermodynamic work of adhesion w_A for most of the systems studied, provided that the metal surface are considered atomically clean. Since they are by no means so clean prior to bonding, it is concluded that the epoxy resin itself purges the metal surfaces of low-energy contamination. In the case of one resin/hardener combination, the interfacial bonding greatly exceeded w_A for oxidized metals (and to a lesser extent for gold) and for the oxide surfaces failure was cohesive. In these cases it is suggested that excess epoxy rings react with the hydrated metal or oxide surfaces to form strong ether-type linkages.

Acknowledgements

Thanks are due to the Science Research Council for support of this work and to the Shell Chemical Company for the provision of adhesive materials.

References

1. E. H. ANDREWS and A. J. KINLOCH, *Proc. Roy. Soc. Lond. A* **332** (1973) 385.
2. *Idem, ibid* **332** (1973) 401.
3. *Idem, J. Polymer Sci. A 2* **11** (1973) 269.
4. *Idem, J. Polymer Sci. C* **46** (1974) 1.
5. E. H. ANDREWS, *J. Mater. Sci.* **9** (1974) 887.
6. S. N. MUCHNICK, US Air Force WADC Tech. Report 55–87 Part II (1958).
7. CIBA-GEIGY, Manual No. A15 g (1971).
8. A. N. GENT and A. J. KINLOCH, *J. Polymer Sci. A 2* **9** (1971) 659.
9. D. M. MATTOX, *J. Vac. Sci. Tech.* **11** (1) (1974) 474, and Report No. 74-0344 (1975) Sandia Laboratories, New Mexico.
10. E. H. ANDREWS and N. E. KING, to be published.
11. S. BEREDAY, Brit. Patent Spec. No. 1339917 (1973) p. 5.
12. W. D. HARKINS and E. H. LOESNER, *J. Chem. Phys.* **18** (1950) 556.
13. D. H. KAELBLE, *J. Adhesion* **2** (1970) 66.
14. W. A. ZISMAN, *Encyclop. Polym. Sci. & Tech.* **1** (1964) 450.
15. G. J. LAKE and A. G. THOMAS, *Proc. Roy. Soc. Lond. A* **300** (1967) 108.
16. W. D. BASCOM, C. O. TIMMONS and R. L. JONES, *J. Mater. Sci.* **10** (1975) 1037.
17. J. J. BICKERMAN, "The Science of Adhesive Joints", 2nd Edn. (Academic Press, New York, 1968).
18. W. R. MACDONALD and K. E. HAYES, *J. Catalysis*, **18** (1970) 115.
19. N. E. KING, Ph.D Thesis, University of London (1976).

Received 23 March and accepted 7 May 1976.